2022 IEEE 5th International Conference on Soft Robotics (RoboSoft)
April 4-8, 2022, Edinburgh, UK

Design, Characterization, and Dynamic Modeling of BEAST: a Bistable Elastomeric Actuator for Swift Tasks

Weijia Tao, Zhi Qiao, and Wenlong Zhang*

***Abstract*— Recent work in fluid-driven soft robots has demonstrated the potential to achieve high power-to-weight ratios, low fabrication costs, and improved safety, making them well suited for interactive tasks. However, the low speed of pneumatic actuation prevents use of these robots in more dynamic tasks. This paper aims to design, characterize, and model a bistable elastomeric actuator for swift tasks (BEAST). This actuator enables both fast actuation and mechanical compliance, and is designed by integrating silicone and polyethylene terephthalate (PET) in a bendy straw structure. The BEAST contains three states - *compressed*, *natural*, and *stretched* states. Two operation modes - *compressed* and *stretched* modes, are defined to model the continuous elongation dynamics before and after the quickly switching around the *natural* state. A set of design rules and a novel fabrication method are presented to develop the BEAST. The actuator characterization shows that the maximum extension ratio, snapping speed, and output force of the BEAST to be 0.58, 1.5m/s, and 48N, respectively. A hybrid linear parameter varying (HLPV) model is developed to describe the pressure-dependent dynamics of the actuator. The actuators are evaluated in an object sorting task where both fast and gentle behaviors are demonstrated.**

I. INTRODUCTION

Soft actuators can conform to objects with different shapes and sizes, and are safe for interacting with humans, thanks to their compliant nature. Among different types of soft actuators, fluid-driven soft actuators have shown advantages such as being low-cost, compact, and customizable [1]. These actuators have been widely adopted in manipulators [2], wearable robots [3], and grippers [4]. However, one critical challenge in fluid-driven soft actuators is their slow actuation speed, which reduces the task efficiency and greatly limits their applications [5].

In order to improve the actuation speed, various approaches have been proposed such as using fast-switching valves with high airflow rates [6] and reducing the chamber volume [7], [8]. For example, an inflatable beam actuator takes around 3 seconds to reach the desired pressure, while another actuator with the same diameter but shorter length takes only 0.68s without performance degradation [7]. However, this method is not scalable since the volume of actuators cannot be arbitrarily decreased. Even with a relatively high airflow rate and small volume, the reaction time of pneumatic actuators is still limited by their slow dynamics.

As an alternative approach, bistable and elastic energy storage structures have been introduced to improve the actuation speed [9]. The bistable structure has two types of equilibrium states (i.e. one unstable state and two stable states) and two local minima of the total potential energy stored in the structure [10]. During the transition from one stable state to the other, the bistable structure will reach the unstable equilibrium state where a small perturbation can drive it to one of the two stable states. When transitioning from an unstable state to a stable one, the system can quickly release a considerable amount of energy. The quick energy release is caused by its negative stiffness near the unstable equilibrium state, and it is also referred as snap-through or buckling [11].

Bistable structures have been used to generate periodic motion such as crawling [12], jumping [13], and grasping [14][15]. In [16], a bistable structure has been successfully employed to achieve fast-speed ground and underwater locomotion, as well as a soft gripper with tunable stiffness. The bendy straw structure is one of the popular bistable structures. It only requires a thin shell to achieve bistability and consists of two frustums that share the same base circle but with different base angles. This unique feature also allows these structures to be easily stacked in series. A single unit of the bendy straw is analyzed in [17], which explains how such a bistable structure holds its shape. Applications of the bendy straw structure include force absorbance due to its negative stiffness and shape morphing when putting multiple of those structures in parallel [18]. Although bistable structures can greatly improve the actuation speed, the actuators cannot deform continuously and are not capable of generating sophisticated motion profiles.

Due to the nonlinear material properties and the bistable behaviors, it is challenging to design accurate dynamic models for the bistable soft actuators. A hybrid dynamic model was proposed for a bistable soft gripper where the authors assumed a constant spring coefficient, and a geometric-based function was utilized as the guards of transitions between the grasping and releasing models [19]. In our previous work [20], it was found that the spring and damping coefficients of the inflatable silicone actuator were linearly dependent on its control input (i.e. the actuator pressure) and the dynamics of this input-dependent system can be described using a linear parameter-varying (LPV) model. However, there is limited work integrating the switching dynamics with the LPV models to describe the dynamics of soft actuators with

This work was supported by the National Science Foundation under Grant CMMI-1800940.

W. Tao and W. Zhang are with The Polytechnic School, Ira A. Fulton Schools of Engineering, Arizona State University, Mesa, AZ, 85212, USA. Email: {wtao11,wenlong.zhang}@asu.edu

Z. Qiao is with the School for Engineering of Matter, Transport, and Energy, Arizona State University, Tempe, AZ, 85287, USA. Email: zqiao7@asu.edu

*Address all correspondence to this author.

2022 IEEE 5th International Conference on Soft Robotics (RoboSoft) | 978-1-6654-0828-8/22/$31.00 ©2022 IEEE | DOI: 10.1109/ROBOSOFT54090.2022.9762223

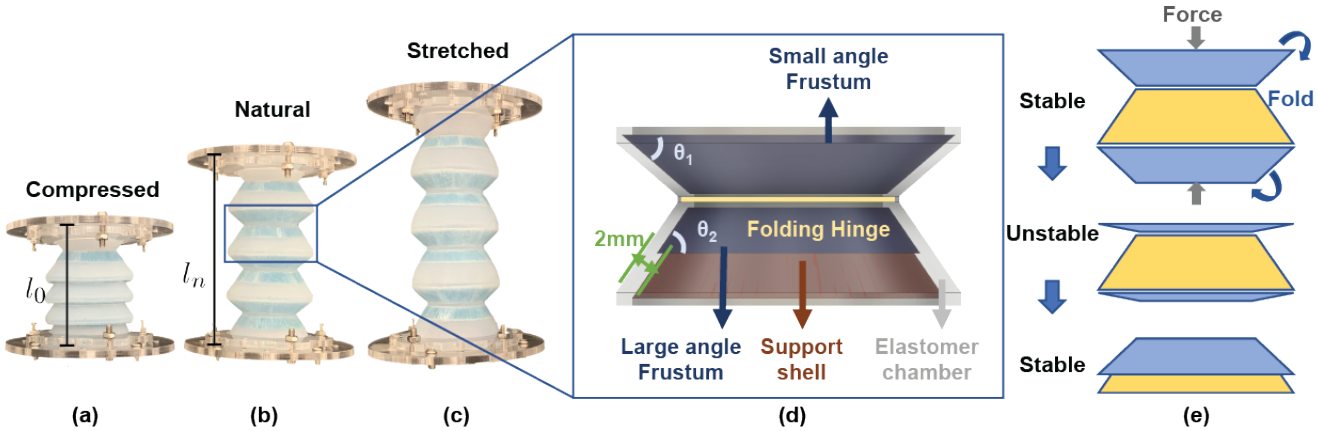

Fig. 1. Actuator overview. (a) *Compressed* state of actuator where l_0 is its minimum length. (b) *Natural* state of actuator with length l_n (c) *Stretched* state of actuator. (d) Single segment of the BEAST, θ_1 and θ_2 are base angles of the frustums. θ_1 is smaller than θ_2. (e) Bistable mechanism of BEAST.

bistable properties.

This paper proposes a novel bistable elastomeric actuator for swift tasks (BEAST) that reacts quickly through a bistable structure while preserving compliance, tunable stiffness with pressure, and continuous elongation capability. Given a pressure input, the BEAST can snap-through quickly to a point close to the desired location. Afterward, it can still make fine adjustments with a continuous motion for precise and compliant manipulation. The pressure to trigger the snapping motion and the continuous motion range is tunable by changing the design parameters. By combining multiple actuators in different configurations, more sophisticated motion patterns could be achieved such as bidirectional bending. Characterization experiments show that a BEAST prototype can achieve a maximum actuation speed of 1.5m/s, a maximum extension ratio at 0.58, and it can generate an output force up to 48N. A hybrid linear parameter varying model (HLPV) is proposed to describe the dynamics of the actuator. A separate LPV model is identified for the *compressed* mode to the *stretched* mode, respectively. In each LPV model, the spring, damper, and pneumatic coefficients are linearly dependent on the input signal. A comparison between the simulation results and the experimental data shows that the HLPV model can accurately describe the dynamics of the BEAST. An application that connected two actuators in parallel performs swift elongation and bending, and is able to perform both power push and a gentle push on an object.

In summary, this work contributes

- The first bistable actuator design with the capability of both fast snap-through and controllable continuous elongation.
- A reliable fabrication approach for embedding polyethylene terephthalate (PET) sheet into silicone rubber.
- An experimentally-validated HLPV model to desrcibe the actuator dynamics.

The remainder of the paper is organized as follows: Section II discusses the design and fabrication of the BEAST. Section III presents the actuator characterization procedure and the experimental results. Section IV introduces the HLPV model for the actuator and the simulation results of the HLPV model. Section V presents the applications with the BEAST. Section VI concludes the paper and discusses the future work.

II. ACTUATOR DESIGN AND FABRICATION

The BEAST is designed to achieve fast snap-through elongation through a bistable structure and continuous axial elongation with an elastomer-made air chamber. As shown in Fig. 1(a-c), it has three states: *compressed* state, *natural* state, and *stretched* state. With the application of triggering pressure, the BEAST quickly snaps from the *compressed* state to the *stretched* state, and keeps extending as the pressure increases. When the supplied pressure returns to the atmosphere level, the BEAST stays in the *natural* state. When a negative pressure is applied, it can return to the *compressed* state. The combination of such functions challenges in geometry design, material selection, and the fabrication process.

A. Actuation Mechanism and Design Requirements

The bistable structure used in the BEAST is similar to a flexible straw consisting of multiple pairs of frustums stacked in series. The overall bistable structure has multiple stable equilibria since it can be fully or partially snapped. As shown in Fig. 1(d), each pair of frustums consists of two thin frustum shells sharing the same base circle diameter: one with a large base angle and one with a small base angle. There is a soft folding hinge where the two frustum shells are connected. As shown in Fig. 1(e), when an axial force is applied to a pair of frustums with different base angles, the one with the small base angle will be triggered first and snaps around the folding hinge. During this process, the structure first turns from one stable state to an unstable state and stores energy. Then it release energy rapidly from the unstable state to another stable state. The frustum with a large base angle only acts as a supporting structure. The force needed for triggering the snapping is proportional to the frustum's base angle and material's Young's modulus [21]. This unique feature enables the fast snap-through discrete elongation/compression behaviors of the actuator. When an

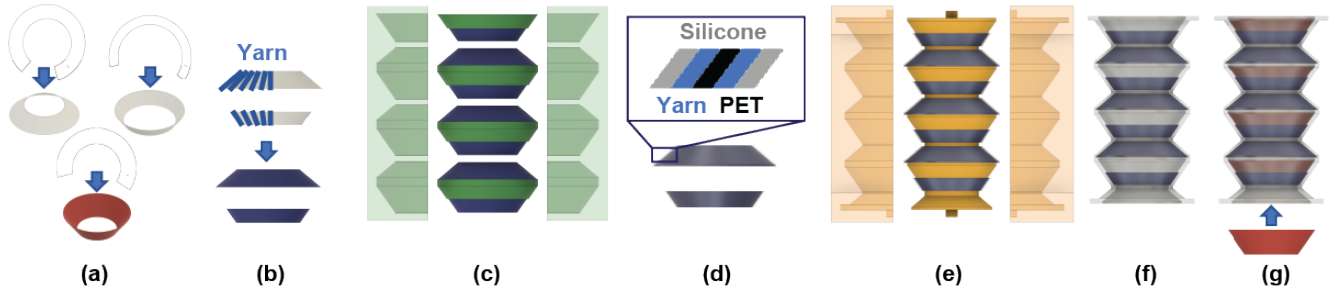

Fig. 2. The manufacturing process of the BEAST. (a) Fold polyethylene terephthalate (PET) sheet into frustum shape. (b) Thread yarn around the PET sheet. (c) Mold PET frustums with silicone. (d) Silicone frustum with embedded PET. (e) Use a different mold with soft thermoplastic polyurethane (TPU) inner mold to combine frustums into actuator shapes. (f) Demold actuator. (g) Insert the PET support shell.

uneven force is applied to the aforementioned pair of frustums, the smaller one will partially fold to the larger one, leading to a bending motion [21]. The *natural* state of the actuator can be adjusted by stacking the different numbers of pairs of frustums in series.

To perform elongation when pressurized, an elastomer material is required to form the air chamber and be embedded with the bistable structure. The elastomer needs to have a high extension ratio and endure high pressure without blasting at relatively thin thickness. When stacking multiple pairs, instead of directly connecting two pairs with a cylindrical elastomer chamber, part of the frustum shell with the large base angle can be shaved off and replaced by elastomer, as shown in Fig. 1(d). In this way, the ratio between the actuator lengths in the *stretched* and *compressed* states increases, and the snapping behavior still exists due to the remaining shell. In addition, elastomer also serves as the soft hinge between the frustum shells.

To maintain both the capability of elongation and retraction, a thin support shell is required for the elastomer wall of the frustum shell with the large base angle to prevent the elastomer material from deforming, presented in Fig. 1(d). Otherwise, the actuator cannot return to its original compressed position because the elastomer wall will be sucked inward and take up the space where the frustum shell folds into. The support shell has about the same shape as the frustum shell with a large base angle and is held in place by the shape of the inner wall. It is not embedded into the elastomer to avoid constraining the elastomer's elongation property.

B. Material Selection

Silicone rubber (Dragon Skin Series, Smooth-On, Inc., Pennsylvania) is chosen as the material for the extensible air chamber. It is widely used in actuating soft robots because of its fast and customizable fabrication process and wide range of hardness. It has a relatively high extension ratio and can withstand a relatively high pressure even with a thin wall.

The polyethylene terephthalate (PET) sheet is selected as the material for bistable frustum shells and support shells because it is inextensible, has a suitable Young's modulus, and is available in various thicknesses. It is stiff enough to store the elastic energy to switch quickly between two stable states. It is also thin and flexible enough so that the triggering pressure is not too high to damage the elastomer air chamber. Additionally, it can be laser cut into different shapes easily.

The combination of these materials also requires special attention. The PET sheet does not adhere to silicone rubber well and can even cut through it when deforming. In order to embed the PET shell into the silicone rubber air chamber, the yarn is wrapped around the shell to serve as not only a cover for the sharp edges but also a medium that can attach to the silicone strongly since the gaps between the small fibers of the yarn absorb and lock the silicone.

C. Design and Fabrication

With the above design considerations, the final BEAST prototype has a length of 82mm with 3 pairs of bistable frustum shells and an additional frustum to simplify mounting. It has an outer diameter of 40mm and a wall thickness of 2mm. With a 2mm thickness, the silicone rubber can stand a pressure that is at least 55.16kPa. Moreover, at this diameter to thickness ratio, the wall thickness is relatively thin to create a soft hinge and allows enough folding space for the frustums. The base angles of a pair of frustums are chosen to be 40° and 55°, respectively. The base angle and thickness of the frustum are selected by trial and error so that the triggering pressure is low enough to avoid any significant elongation of the chamber since it is important to have enough continuous elongation range after the snapping. The thickness of the PET sheet and the hardness of the silicone rubber are varied, and their impacts on the actuator's performance are evaluated through experiments, presented in Section III.

The fabrication process is shown in Fig. 2 and there are three main steps: embedding frustum shells into silicone, stacking frustum shell pairs, and inserting support shells. First, the PET sheet is laser cut into three different shapes and folded, and glued into the frustum shells with different base angles and the support shells, presented in Fig. 2(a). Each bistable segment requires a set of three different shells. Then, the frustum shells are threaded with yarn to have a robust bound with silicone, presented in Fig. 2(b). After that, the threaded PET shells are put into a 3D printed mold where silicone is also poured, as shown in Fig. 2(c). Once cured and released, a thin cover of silicone can be applied evenly and robustly on those frustum shells, presented in Fig. 2(d). The next step is to connect the frustum shells

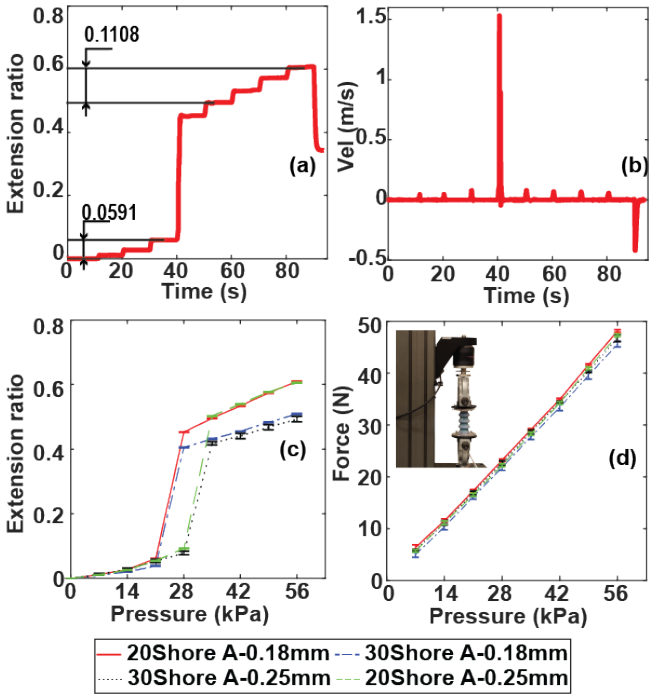

Fig. 3. Experimental results. (a) Extension ratio vs. time for 20Shore A-0.18mm actuator. (b) Elongation velocity vs. time for 20Shore A-0.18mm actuator. (c) Extension ratio vs. input pressure and (d) Output force vs. input pressure for 20Shore A-0.18mm (solid red), 30Shore A-0.18mm (dotted-dashed blue), 30Shore A-0.25mm (dotted black) and 20Shore A-0.25mm (dashed green) actuators.

together with silicone in another 3D printed mold, as shown in Fig. 2(e). A 3D printed soft deformable inner mold is used to hold the frustum shells so that they can be squeezed and pulled out during demolding. As shown in Fig. 2(g), the final step is to insert the PET support shells into the demolded actuator (Fig. 2(f)). It should be noted that embedding the yarn-threaded frustum shells into silicone rubber can result in many air gaps that cause leaking. Therefore, individual frustum shells have to be made first and then molded again to better fill those gaps. To create an airtight seal for the BEAST's top and bottom as well as enable pressure input, acrylic plates with vent screw-mounted are used to clamp the silicone [22], shown in Fig. 1.

III. CHARACTERIZATION

A. Elongation Performance

We evaluated the performance of the BEAST by changing the hardness value of silicone and the thickness of the PET. The hardness was changed from 20 to 30Shore A, and the thickness was varied from 0.18mm to 0.25mm, resulting in four different actuator designs.

A motion test was conducted for each parameter set utilizing a motion capture system with six cameras (Optitrack, NaturualPoint Inc., Corvallis, OR). The goal of the motion test was to evaluate the relationship between the input pressure and the actuator's extension ratio. The actuator was mounted on a rigid plate while the input air pressure was changed from 0kPa to 55.16kPa, with 6.89kPa increments. Markers were placed on the bottom and top plates of the actuator. The marker positions were recorded at 120Hz through the motion capture system. For each actuator, the motion test was repeated three times, and the results are presented in Fig. 3 where the extension ratio η is defined as:

$$\eta = \frac{h}{l_0} \tag{1}$$

where l, l_0, and $h = l - l_0$ are the actual length, the minimum *compressed* state length, and the length changes of the BEAST.

Figure 3(a) presents the extension ratio changes of a 20Shore A-0.18mm actuator when the input pressure changes from 0kPa to 55.16kPa. A snapping motion is observed around 40 seconds since the desired pressure 27.58kPa is larger than the triggering pressure of the actuator. It is also observed that the actuator dynamics changes with the occurrence of snapping motion, since the exact pressure increment results in different extension ratio increases (e.g., 0.0591 with 0kPa to 20.68kPa vs. 0.1108 with 34.47kPa to 55.16kPa). Therefore, at least two different models are required to describe the dynamics of the actuator. As presented in Fig. 3(b), the maximum speed of the snapping motion is 1.5m/s, which indicates that the BEAST can achieve large length changes in a short time interval.

Figure 3(c) compares the behaviors of the actuators with different silicone hardness and PET thickness. The exact pressure increment is applied to all four actuators, three times each. The 20 Shore A actuators (solid red and dashed green) show higher extension ratios when comparing different silicone hardness, and it also shows that the PET thickness does not affect the extension ratio. Since the PET sheet is inextensible, harder silicone rubber deforms less under the same pressure input. The 0.25mm actuators (dotted black and dashed green) present higher triggering pressure, and it indicates that the PET thickness has a more significant effect on triggering pressure than the silicone hardness. Since PET has a much higher Young's modulus, the hardness change of the silicone rubber has little effect on the overall stiffness of the frustums.

B. Output Force Evaluation

We also investigated the relationship between the output force from the actuator and the input pressure through experiments. The experiments were performed on a Universal Tensile Machine (Instron 5944; Instron Crop., High Wycombe, UK). The actuator was fixed at the *natural* state during the experiment, and the external force was measured for the same input air pressure profile mentioned in the motion test.

Figure 3(d) compares the output force of the actuators with different silicone hardness and PET thickness. With a maximum operating pressure of 68.95kPa, the input pressure is changed from 0kPa to 55.16kPa for the safety concern, and the exact pressure increment is applied to all four actuators three times. It is observed that the PET sheet thickness and silicone rubber hardness do not affect the actuator's force output at the *natural* state because all actuators tend

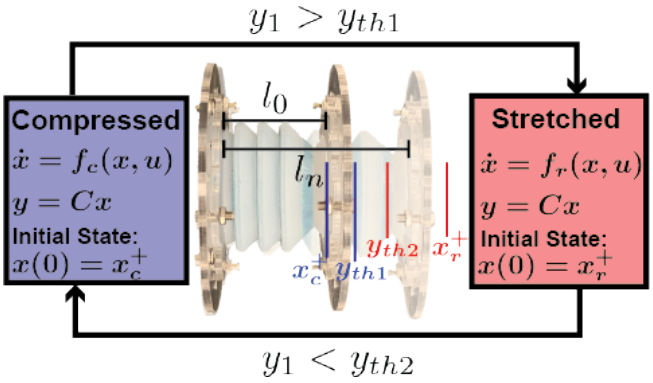

Fig. 4. A hybrid linear parameter-varying (LPV) model for the BEAST.

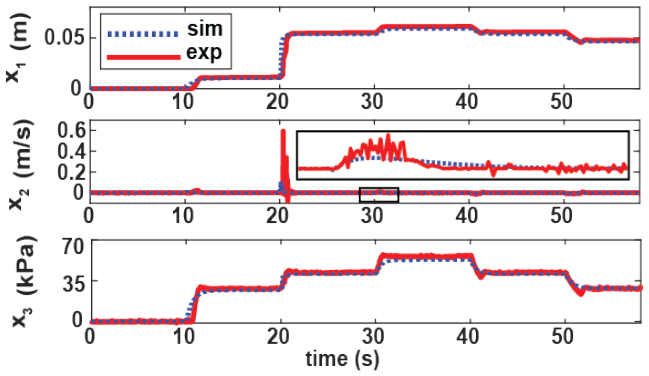

Fig. 5. HLPV model validation. x_1, x_2, and x_3 are the length changes, the elongation velocity, and measured pressure. The simulation (dashed blue) matches the experimental results of the 20*Shore A*-0.25mm actuator (solid red).

to elongate along the axial direction while the contacting surface areas are not changed. It is also noted that the actuator can generate up to 48N pushing force along the axial direction.

IV. DYNAMIC MODELING

A. HLPV Model of the Bistable Actuator

Since the exact pressure increment results in different extension ratio increases, as presented in Fig. 3(a), we extend our previous work [20] and propose an input-dependent HLPV model for the system, which incorporates the dynamics of both the actuator and the pressure controller. As presented in Fig. 4, two operation modes: *compressed* and *stretched* are defined to model the continuous elongation dynamics before and after the *natural* state. The snapping condition y_{th1} and the initial state x_r^+ were evaluated experimentally. It should be noted that the frustums cannot achieve the snapping motion simultaneously due to the fabrication errors. So, the other snapping condition, y_{th2} was calculated as absolute value of the difference between the length at *natural* state and the height of one smaller-angled frustum . Although a vacuum pump was utilized to drive the actuator snapping from the *stretched* mode to the *compressed* mode, regulating negative pressure value is outside the scope of this paper. Therefore, the initial state x_c^+ is selected as the *compressed* state with minimum length, zero velocity, and atmospheric pressure. The dynamic model of the two modes are as follows:

$$f_c(x,u) = \begin{bmatrix} x_2 \\ -\frac{k_c(u)}{m}x_1 - \frac{b_c(u)}{m}x_2 + \frac{\gamma}{m}x_3 \\ \alpha_c(u)x_3 + \beta_c(u)u \end{bmatrix}$$

$$f_r(x,u) = \begin{bmatrix} x_2 \\ -\frac{k_r(u)}{m}(x_1 - h_n) - \frac{b_r(u)}{m}x_2 + \frac{\gamma}{m}x_3 \\ \alpha_r(u)x_3 + \beta_r(u)u \end{bmatrix}$$

$$C = \begin{bmatrix} 1 & 0 & 0 \\ 0 & 0 & 1 \end{bmatrix} \quad (2)$$

where

$$x = [h, \dot{h}, p_m]^T, \; h_n = l_n - l_0$$

m, u, l_n, and p_m are the mass, input pressure set-point, *natural* state length, and the air pressure inside the chamber of the actuator. $k(u), b(u), \alpha(u)$, and $\beta(u)$ are the input-dependent parameters. $\gamma = 5.577$ is the coefficient that maps the chamber's air pressure to the output force and it is identified through the aforementioned payload test, as shown in Section III-B.

In order to identify the parameters (i.e., $k(u), b(u), \alpha(u)$, and $\beta(u)$) for each mode, we excited the system with two series of step inputs. For the *compressed* mode, the pressure setpoint was changed from 0kPa to 27.58kPa, with increments of 6.89kPa where the triggering pressure of the snapping motion was 34.9kPa. For the *stretched* mode, the system was first elongated to the *natural* state. Then the pressure set-point was changed from 0kPa to 55.16kPa, with increments of 6.89kPa. For each trail, the actuator was first inflated to the pressure setpoint for 10 seconds then it was deflated to 0kPa for another 10 seconds. Three trials were recorded for each pressure set-point, and thirty-six trials in total were recorded. We utilized MATLAB to estimate the parameters for each input pressure set-point and then identify the polynomial function to express the relationship between the input pressure and each parameter.

B. HLPV Model Validation

As a preliminary study, we only utilize one input profile to identify the model switching conditions and validate the model performance. The switching conditions, presented in Fig. 4, are $y_{th1} = 0.01406$ and $y_{th2} = 0.027$ and the initial conditions are $x_r^+ = [0.0447, 0.1067, 5.6]^T$ and $x_c^+ = [0,0,0]^T$. As presented in Fig. 5, the simulation results from the proposed model match the experimental data very well. It confirms that the HLPV model can accurately describe the changes in the actuator length and the air pressure within the chamber.

V. APPLICATION: OBJECT SORTING

The developed actuators can be connected to perform different tasks, such as object sorting and manipulation. In this section, we present one example that shows the capability of two identical actuators connected in parallel. In a sorting task, it is important to quickly push objects to the desired location. In the meantime, a gentle push is

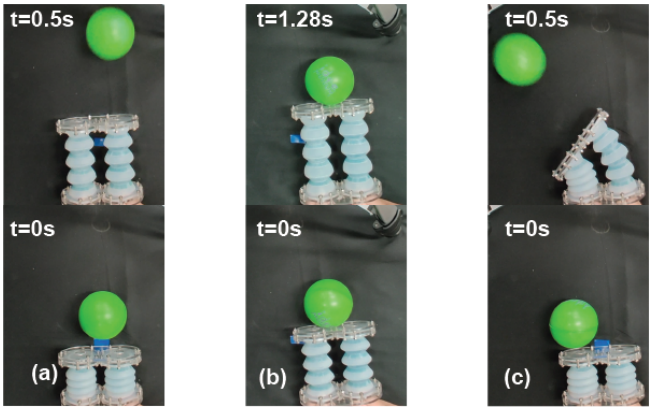

Fig. 6. Screenshots of the video for object pushing application. (a) Power push to the front. (b) A gentle push to the front. (c) Power push to the side. The full video is attached to the supplementary material.

required to not damage some fragile objects. This BEAST module can perform a power push of a stress ball to its front and side by applying pressure when it is at the *compressed* state (Fig. 6(a), (c)). It can also gently push the object by applying pressure when it is at the *natural* state (Fig. 6(b)). A video demonstrating the developed soft actuators can be found at `https://youtu.be/4QxHrXKJn4M`. More sophisticated object manipulation tasks could be achieved by connecting multiple BEASTs in parallel and series.

VI. CONCLUSIONS

This work proposed a BEAST that can perform snap-through fast elongation through bistable structures as well as operate as a conventional linear actuator. It can perform a maximum snapping speed of 1.5m/s and elongate for an additional 20 percent afterward. Through varying its bistable material PET sheet and soft material silicone rubber, the actuator's triggering pressure and deformation range can be tuned. Its large extension ratio and fast reaction time were further demonstrated in an object push application scenario. An HLPV model was proposed to describe the dynamics of the actuator. Two LPV models, in total, were utilized for the *compressed* and the *stretched* modes, respectively. The parameters of each LPV model were individually identified through different sets of experiments. Simulation results showed that the HLPV model was able to accurately describe the dynamics of the actuator.

Future work will explore the possibility of achieving multiple snapping lengths through combining frustums of different triggering pressures, which could greatly increase the workspace for this actuator. The extra deformation capability after the snapping will also be used in robotic applications that require a fast approach but precise force or pose control. An example could be the portable arm for drones to pick and place objects. A more dynamical input profile will be applied to the actuator to improve the HLPV model performance, and a model-based feedback controller will also be designed to close the position control loop. In addition, a soft robot with multiple actuators connected in parallel and series will be developed for more sophisticated tasks such as whole-body grasping.

REFERENCES

[1] P. Polygerinos, N. Correll, S. A. Morin, B. Mosadegh, C. D. Onal, K. Petersen, M. Cianchetti, M. T. Tolley, and R. F. Shepherd, "Soft Robotics: Review of Fluid-Driven Intrinsically Soft Devices; Manufacturing, Sensing, Control, and Applications in Human-Robot Interaction," *Advanced Engineering Materials*, vol. 19, no. 12, 2017.

[2] P. H. Nguyen, I. I. Mohd, C. Sparks, F. L. Arellano, W. Zhang, and P. Polygerinos, "Fabric soft poly-limbs for physical assistance of daily living tasks," *Proc. IEEE Int. Conf. on Robotics and Automation*, pp. 8429–8435, 2019.

[3] P. H. Nguyen and W. Zhang, "Design and computational modeling of fabric soft pneumatic actuators for wearable assistive devices," *Scientific reports*, vol. 10, no. 1, pp. 1–13, 2020.

[4] Y. Hao, Z. Gong, Z. Xie, S. Guan, X. Yang, Z. Ren, T. Wang, and L. Wen, "Universal soft pneumatic robotic gripper with variable effective length," *Proc. Chinese Control Conference*, vol. 2016-August, pp. 6109–6114.

[5] C. Laschi and M. Cianchetti, "Soft robotics: New perspectives for robot bodyware and control," *Frontiers in Bioengineering and Biotechnology*, vol. 2, no. JAN, pp. 1–5, 2014.

[6] E. E. Topçu, I. Yüksel, and Z. Kamiş, "Development of electro-pneumatic fast switching valve and investigation of its characteristics," *Mechatronics*, vol. 16, no. 6, pp. 365–378, 2006.

[7] S. Sridar, S. Poddar, Y. Tong, P. Polygerinos, and W. Zhang, "Towards Untethered Soft Pneumatic Exosuits Using Low-Volume Inflatable Actuator Composites and a Portable Pneumatic Source," *IEEE Robotics and Automation Letters*, vol. 5, no. 3, pp. 4062–4069, 2020.

[8] D. Hutmacher, B. Gorissen, S. Liponsky, and T. Shabab, "Ultrafast Soft Actuators," *ResearchSquare*, pp. 1–16, 2021.

[9] A. Pal, V. Restrepo, D. Goswami, and R. V. Martinez, "Exploiting Mechanical Instabilities in Soft Robotics: Control, Sensing, and Actuation," *Advanced Materials*, vol. 2006939, p. 2006939, 2021.

[10] Y. Chi, Y. Li, Y. Zhao, Y. Hong, Y. Tang, and J. Yin, "Bistable and Multistable Actuators for Soft Robots: Structures, Materials, and Functionalities," *Advanced Materials*, vol. 2110384, p. 2110384, 2022.

[11] C. S. Ha, R. S. Lakes, and M. E. Plesha, "Design, fabrication, and analysis of lattice exhibiting energy absorption via snap-through behavior," *Materials and Design*, vol. 141, pp. 426–437, 2018.

[12] K. Gustafson, O. Angatkina, and A. Wissa, "Model-based design of a multistable origami-enabled crawling robot," *Smart Materials and Structures*, vol. 29, no. 1, 2020.

[13] B. Gorissen, D. Melancon, N. Vasios, M. Torbati, and K. Bertoldi, "Inflatable soft jumper inspired by shell snapping," *Science Robotics*, vol. 5, no. 42, pp. 1–8, 2020.

[14] A. K. Nguyen, A. Russell, N. Naclerio, V. Vuong, H. Huang, K. Chui, and E. W. Hawkes, "A Tri-Stable Soft Robotic Finger Capable of Pinch and Wrap Grasps," *Proc. IEEE Robotics and Automation*, pp. 9028–9034, 2020.

[15] T. G. Thuruthel, S. Haider Abidi, M. Cianchetti, C. Laschi, and E. Falotico, "A bistable soft gripper with mechanically embedded sensing and actuation for fast grasping," *Proc. IEEE Int. Conf. on Robot and Human Interactive Communication*, pp. 1049–1054, 2020.

[16] Y. Tang, Y. Chi, J. Sun, T.-H. Huang, O. H. Maghsoudi, A. Spence, J. Zhao, H. Su, and J. Yin, "Leveraging elastic instabilities for amplified performance: Spine-inspired high-speed and high-force soft robots," *Science advances*, vol. 6, no. 19, p. eaaz6912, 2020.

[17] N. P. Bende, T. Yu, N. A. Corbin, M. A. Dias, C. D. Santangelo, J. A. Hanna, and R. C. Hayward, "Overcurvature induced multistability of linked conical frusta: How a 'bendy straw' holds its shape," *Soft Matter*, vol. 14, no. 42, pp. 8636–8642, 2018.

[18] F. Pan, Y. Li, Z. Li, J. Yang, B. Liu, and Y. Chen, "3D Pixel Mechanical Metamaterials," *Advanced Materials*, vol. 31, no. 25, pp. 1–8, 2019.

[19] J. McWilliams, Y. Yuan, J. Friedman, and C. Sung, "Push-on push-off: A compliant bistable gripper with mechanical sensing and actuation," in *Proc. IEEE Int. Conf. on Soft Robotics*, 2021, pp. 622–629.

[20] Z. Qiao, P. H. Nguyen, P. Polygerinos, and W. Zhang, "Dynamic modeling and motion control of a soft robotic arm segment," in *Proc. American Control Conference*, 2019, pp. 5438–5443.

[21] B. Zhang, "Bistable and multi-stable thin-walled structures," Ph.D. dissertation, University of Oxford, 2017.

[22] W. Tao, E. H. Skorina, F. Chen, J. McInnis, M. Luo, and C. D. Onal, "Bioinspired design and fabrication principles of reliable fluidic soft actuation modules," *Proc. IEEE Int. Conf. on Robotics and Biomimetics*, pp. 2169–2174, 2015.